

POLITECNICO DI TORINO  
Repository ISTITUZIONALE

Year-long optical time scale with sub-nanosecond capabilities

*Original*

Year-long optical time scale with sub-nanosecond capabilities / Formichella, V., Signorile, G., Thai, T.T., Galleani, L., Pizzocaro, M., Goti, I., Condio, S., Clivati, C., Risaro, M., Levi, F., Calonico, D., Sesia, I.. - In: OPTICA. - ISSN 2334-2536. - ELETTRONICO. - 11:4(2024), pp. 523-530. [10.1364/OPTICA.509706]

*Availability:*

This version is available at: 11583/2993133 since: 2024-10-07T15:53:06Z

*Publisher:*

Optica Publishing Group

*Published*

DOI:10.1364/OPTICA.509706

*Terms of use:*

This article is made available under terms and conditions as specified in the corresponding bibliographic description in the repository

*Publisher copyright*

Optica Publishing Group (formely OSA) postprint versione editoriale con OAPA (OA Publishing Agreement)

© 2024 Optica Publishing Group. Users may use, reuse, and build upon the article, or use the article for text or data mining, so long as such uses are for non-commercial purposes and appropriate attribution is maintained. All other rights are reserved.

(Article begins on next page)



# Year-long optical time scale with sub-nanosecond capabilities

VALERIO FORMICHELLA,<sup>1</sup>  GIOVANNA SIGNORILE,<sup>1</sup>  TUNG THANH THAI,<sup>1</sup>   
LORENZO GALLEANI,<sup>2</sup>  MARCO PIZZOCARO,<sup>1</sup>  IRENE GOTI,<sup>1,2</sup>  STEFANO CONDIO,<sup>1,2</sup>   
CECILIA CLIVATI,<sup>1</sup>  MATIAS RISARO,<sup>1</sup>  FILIPPO LEVI,<sup>1</sup>  DAVIDE CALONICO,<sup>1</sup>  AND  
ILARIA SESIA<sup>1,\*</sup> 

<sup>1</sup>Quantum Metrology and Nanotechnologies Division, INRiM, Turin, Italy

<sup>2</sup>Department of Electronics and Telecommunications, Politecnico di Torino, Turin, Italy

\*i.sesia@inrim.it

Received 19 October 2023; revised 28 February 2024; accepted 10 March 2024; published 17 April 2024

An atomic time scale is a method for marking events and the passage of time by using atomic frequency standards. Thanks to the superior performance of atomic clocks based on optical transitions, time scales generated with optical clocks have the potential to be more accurate and stable than those based on microwave clocks. In this work, we demonstrate an experimental optical time scale based on the INRiM Yb optical lattice clock and a hydrogen maser as a flywheel oscillator, showing sub-nanosecond accuracy over months-long periods and nanosecond accuracy over a 1-year period. The obtained results show that optical time scales have competitive performances even when the optical clock has a limited and non-uniformly distributed up-time. Consequently, we are working to include the Yb clock within the ensemble of clocks routinely used for the generation of the Italian time scale. Furthermore, these results represent a crucial step towards the future redefinition of the second of the International System of Units based on an optical transition. © 2024

Optica Publishing Group under the terms of the [Optica Open Access Publishing Agreement](#)

<https://doi.org/10.1364/OPTICA.509706>

## 1. INTRODUCTION

The last two decades have seen the development and constant improvement of optical frequency standards, based on different species of neutral atoms and ions whose accuracy and stability surpass by orders of magnitude those of the best available microwave Cs clocks, which presently realize the second in the International System of Units (SI) [1–3]. On one hand, the performance of optical frequency standards has been exploited for fundamental physics experiments, such as chronometric geodesy and the search for time-variations of fundamental constants [4–6]. On the other hand, the optical transitions on which they are based are excellent candidates for a future redefinition of the SI second [7,8], as also highlighted in Resolution 5 of the 27th meeting of the General Conference on Weights and Measures held in November 2022 [9]. One recognized requirement for the redefinition is the incorporation of optical frequency standards into existing time scales, which are methods for marking events and the passage of time. For instance, Coordinated Universal Time (UTC), the international reference time scale recommended for civil use [10,11], has recently started incorporating optical clocks as secondary representations of the second [12,13], alongside primary frequency standards like Cs fountains. Moreover, several recent works theoretically and experimentally demonstrate the inclusion of optical clocks as reference for the generation of time scales based on a flywheel oscillator ensuring continuous operation, such as an H

maser [14–19], or on an ultra-stable cavity [20]. One key challenge for the realization of such time scales is that optical frequency standards are typically operated intermittently and do not yet guarantee the same level of robustness and reliability of H masers or Cs fountain primary frequency standards, despite a few demonstrations of optical clocks operated almost continuously [21–24] and for relatively long periods of time [25–27]. Similar constraints come from the capability of a frequency comb, locked to the frequency of an optical clock, to generate a coherent time output for a long time [28]. The accuracy and stability of a continuous time scale based on an optical clock, henceforth called optical time scale (OTS), depend on the stability and predictability of the H maser used as flywheel oscillator, on the availability of the optical clock data, and on the algorithm adopted for OTS generation [29,30]. To incorporate optical clocks into time scales, it is thus urgent to establish hardware and methods that enable the full exploitation of their superior performances while coping with practical constraints that are especially relevant for real-time operations.

In this work, we operate INRiM Yb optical lattice clock IT-Yb1 [31] to generate an OTS for over a year, by using a robust algorithm based on our previous studies [29]. Specifically, we present the results of a paper OTS, i.e., calculated in post-processing, for 12 months of experimental data, from February 2022 to January 2023, and those of a physical OTS, i.e., generated in real-time, for almost 5 months, from December 2022 to April 2023. The

performances of the obtained OTSs are carefully analyzed, with particular attention to the role of the optical clock up-time as compared with those of other OTSs discussed in the referenced literature, and with those of the Italian time scale. The duration of our experiment rivals that of previous ones reported in literature, while reaching similar sub-nanosecond accuracy over months-long periods. Moreover, our experiment shows the capacity to generate an OTS for a significant duration with “only” an H maser, a comb, and an optical lattice clock, thus representing what we believe to be a very concrete step forward for the redefinition of the SI second.

The paper is organized as follows: in Section 2 we give an overview of the experimental setup; in Section 3 we introduce the frequency standards considered in our experiment; in Section 4 we briefly review the robust algorithm for the OTS generation; in Section 5 we present and discuss the results obtained for both the paper and physical OTSs; finally, Section 6 reports on our conclusions.

## 2. EXPERIMENT OVERVIEW

Practical applications need a physical time scale continuously available. As opposed to paper time scales, physical time scales are computed in real-time and provide constantly available physical signals generated by hardware systems. These signals are typically generated by a flywheel oscillator, such as an H maser, whose frequency is “corrected,” or steered, versus a more accurate reference, such as a Cs fountain, through a dedicated algorithm. For example, this is the case for the Italian time scale UTC(IT), the physical realizations of UTC generated in our laboratory.

Figure 1(a) shows a high-level diagram of the INRiM setup used for the generation of UTC(IT) and of the OTS. The generation of UTC(IT) is based on a commercial H maser, whose frequency is measured and steered towards the local Cs fountain (or towards UTC in case of Cs fountain data unavailability). The resulting time scale is then synchronized to UTC by using data from the BIPM [blue blocks in Fig. 1(a)]. The generation of the OTS follows the same approach, but the frequency correction to steer the H maser is

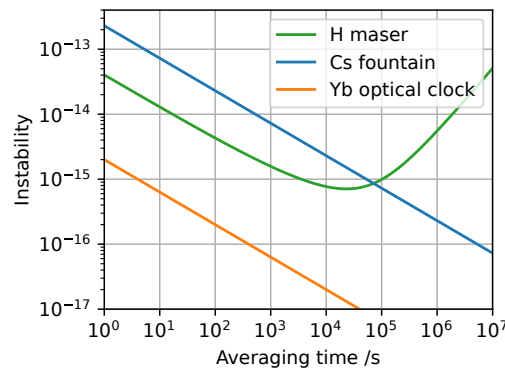
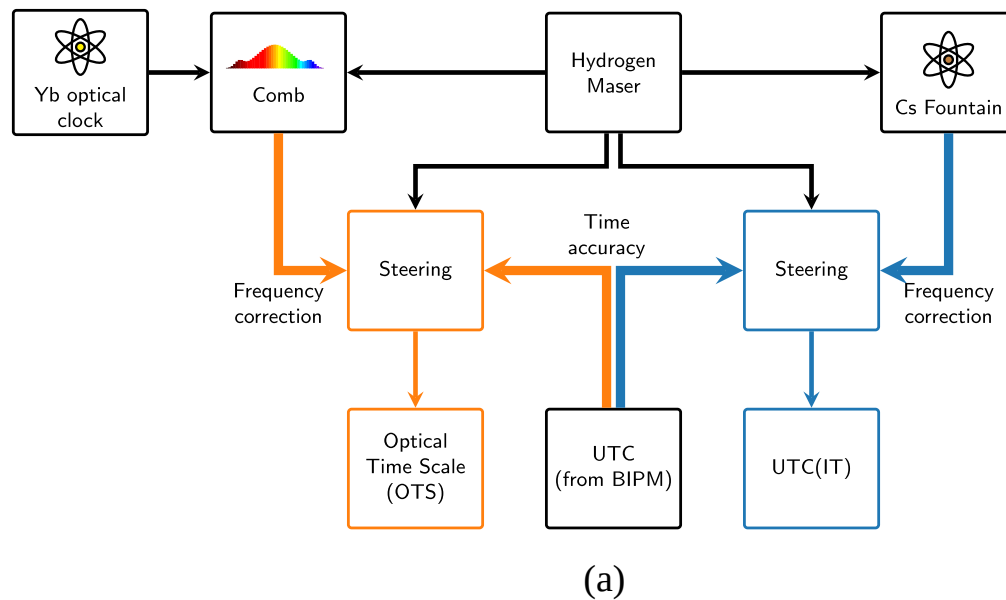


**Fig. 1.** (a) Scheme of the experimental setup for the generation of UTC(IT) and the optical time scale (OTS). Both are generated by steering the frequency of the same H maser. In the generation of UTC(IT), the H maser is directly measured by the local Cs fountain; in OTS generation, the H maser is measured against the Yb optical clock using an optical frequency comb. The steering of UTC(IT) and the OTS uses data from the BIPM to ensure the time accuracy relative to UTC. (b) Typical frequency instability of the H maser, Cs fountain, and Yb optical clock expressed as Allan deviation as a function of averaging time.

derived from the Yb optical clock measured on an optical frequency comb [orange blocks in Fig. 1(a)]. The OTS can be generated both physically (in real time), as is the case of UTC(IT), and as a paper time scale (in post-processing), by using the same input data. The advantage of a paper time scale is that it can also be used to test alternative algorithms or alternative configurations.

A detailed description of the architecture in Fig. 1(a), both from a hardware and software point of view, can be found in Supplement 1, Section 1 and in [32,33].

The main advantage of using an optical clock as a reference for generating a time scale is that its instability is much lower than that of an H maser and a Cs fountain for all averaging times, as can be seen from Fig. 1(b). As a matter of fact, if a time scale is generated by using an H maser and a Cs fountain, the best achievable instability is the one of the H maser at small and medium averaging time (smaller than one day), and the one of the Cs fountain at larger averaging time (greater than one day). This result can be obtained by a proper frequency steering algorithm (such as the one described in Section 4), which corrects the H maser drift, dominating at averaging times larger than one day. Hence, typically, the frequency correction from the Cs fountain is applied once a day. Conversely, if we generate a time scale by using an H maser and an optical clock, the steering algorithm can correct the H maser even by using a few hours only of optical clock measurements, resulting in a much more stable time scale, a quicker reaction to unexpected H maser anomalies, and a more effective drift compensation in the long term.

### 3. FREQUENCY STANDARDS CONSIDERED FOR OUR EXPERIMENT

The H maser used in the experiment is an iMaser 3000 manufactured by T4Science [34], henceforth indicated as HM4 by its code used at INRiM. During the test period, HM4 showed a linear frequency drift of about  $6 \times 10^{-16}$ /day (measured with respect to the Yb clock), a flicker floor smaller than  $1 \times 10^{-15}$ , and a few frequency anomalies, such as instantaneous frequency jumps greater than  $2 \times 10^{-15}$ , which in some commercial H masers can be observed 2–3 times a year.

The  $^{171}\text{Yb}$  optical lattice frequency standard IT-Yb1 has been described in [31,35,36]. The clock laser of IT-Yb1 is stabilized on an ultrastable cavity and interrogates the Yb atoms trapped in an optical lattice. Then, a digital control loop locks the clock laser frequency to the optical transition frequency of the  $^{171}\text{Yb}$  atoms, by acting on an acousto-optic modulator. Finally, the clock laser is sent to a fiber frequency comb referenced to HM4, allowing the comparison between the optical clock and the H maser frequencies. The total relative uncertainty of IT-Yb1 is  $1.9 \times 10^{-17}$ , with a typical instability of  $2 \times 10^{-15}/\sqrt{\tau/s}$  [31]. Usually, excluding longer unavailability periods due to maintenance, upgrades, and unexpected events, IT-Yb1 operated for some hours during working days, in the considered period. IT-Yb1 was run unattended, when possible, albeit with reduced reliability. The raw frequency offset data are pre-processed and averaged to obtain, typically, one or two data points per day, which are then used for the generation of the OTS. Such daily-averaged data are currently made available with a latency ranging from few hours to few days, necessary for their validation so that, for the tests presented in this work, the steering correction is updated and applied once per day.

Each data is given with an associated measurement uncertainty, which enables us to properly weight them within the steering

algorithm. The uncertainty takes into account dead times and the instability contribution of the whole measurement chain. The comb instability contribution is measured by comparison with a second comb to be about  $7 \times 10^{-14}/(\tau/s)^{0.7}$  in terms of Allan deviation (ADEV). At the time of our experiment, the instability of cables distributing the H maser signal to the comb was evaluated to be negligible with respect to the comb contribution. From a more recent assessment, this contribution was conservatively re-evaluated to an ADEV of about  $5 \times 10^{-14}/\sqrt{\tau/s}$ , but, as shown in Supplement 1, Section 4, the updated uncertainty has a negligible impact on our results. This uncertainty can be reduced further by improving the frequency distribution hardware to the comb.

### 4. STEERING ALGORITHM

The goal of this work is not to present a new steering algorithm for the generation of an OTS, but rather to apply a robust steering algorithm that we already developed and published in literature [29,37] (properly tuned to adapt to the up-time of the optical clock), to a state-of-the-art experimental set-up, for the generation of an OTS with unprecedented duration and competitive performances. We now briefly summarize the basic principle of this steering algorithm.

The steering algorithm keeps the H maser frequency in agreement with respect to a more accurate reference. This goal is achieved by regularly applying a frequency correction to the H maser frequency. In our case, the applied frequency steering correction  $\Delta f$  is computed as the sum of three components:  $\Delta f_0$ ,  $\Delta f_1$ , and  $\Delta f_2$ . The main component  $\Delta f_0$  is used to correct the frequency offset of the H maser clock with respect to the chosen reference (in our case, IT-Yb1). The  $\Delta f_0$  component is computed through a linear fit on a batch of frequency data with  $N_{\text{fit}}$  days of length, extrapolated to the epoch in which the correction has to be applied.

The time scale obtained by applying the  $\Delta f_0$  correction can show a residual frequency offset with respect to a reference time scale, such as UTC. This residual frequency offset can be compensated by using the  $\Delta f_1$  component, computed by averaging the residual frequency offset data over a recent period. Note that, for this work, we observed that the residual frequency offset is negligible, being the IT-Yb1 and UTC frequency difference lower than  $2 \times 10^{-16}$  and in agreement with the current definition of the SI second based on Cs; therefore, we set  $\Delta f_1 = 0$ . Finally, the  $\Delta f_2$  component corrects the residual time offset of the realized time scale with respect to the reference time scale, and it is computed by dividing the most recently measured residual time offset by the parameter  $N_{\text{acc}}$ . This parameter represents the desired time interval after which the time offset is reduced to zero. Therefore, the role of  $\Delta f_2$  is to provide time accuracy to the generated time scale, whereas  $\Delta f_0$  accounts for its frequency accuracy.

In case of an UTC(k) time scale realization, the reference for the computation of  $\Delta f_2$  should be UTC. Nevertheless, UTC rapid (UTC<sub>r</sub>), i.e., the rapid version of UTC available weekly, can also be used thanks to its reduced latency and despite its slightly larger instability [38].

In the particular case of an OTS with its potentially superior performance, the choice of the reference time scale must be carefully handled depending on the specific experimental conditions, such as optical clock up-time and flywheel stability. For the experiments discussed in this work, where the up-time is relatively low, the optical clock experiences long unavailability periods, and the

flywheel suffers from some clock anomalies, we select UTCr (see Supplement 1, Section 3, for a performance comparison with UTC).

## 5. EXPERIMENTAL RESULTS

### A. Paper Optical Time Scale Results

The paper OTS results described in this section are based on the HM4 versus IT-Yb1 measurement data collected over 12 months from February 2022 to January 2023. For this test, the  $\Delta f_0$  steering component is obtained with  $N_{\text{fit}} = 30$  days, a choice which improves the steering performances and the stability of the time

scale in nominal conditions, as discussed in [37]. The time accuracy component  $\Delta f_2$  is instead computed from UTCr, by using  $N_{\text{acc}} = 20$  days. As discussed in [37], this choice of  $N_{\text{acc}}$  provides a smooth compensation of the residual OTS time offset, and it maximizes the reactivity of the algorithm to possible deviations from UTCr (see Supplement 1, Section 3, for further details).

Figure 2 shows the results of the obtained paper time scale. Figure 2(a) shows the daily-averaged frequency offset data of HM4 versus IT-Yb1, after removing a linear frequency drift of approximately  $6 \times 10^{-16}$ /day over the whole considered period. Data gaps larger than 2 weeks are indicated by gray-shaded regions. The optical clock up-time, here defined as the percentage of days with at least one measurement within the considered period, is

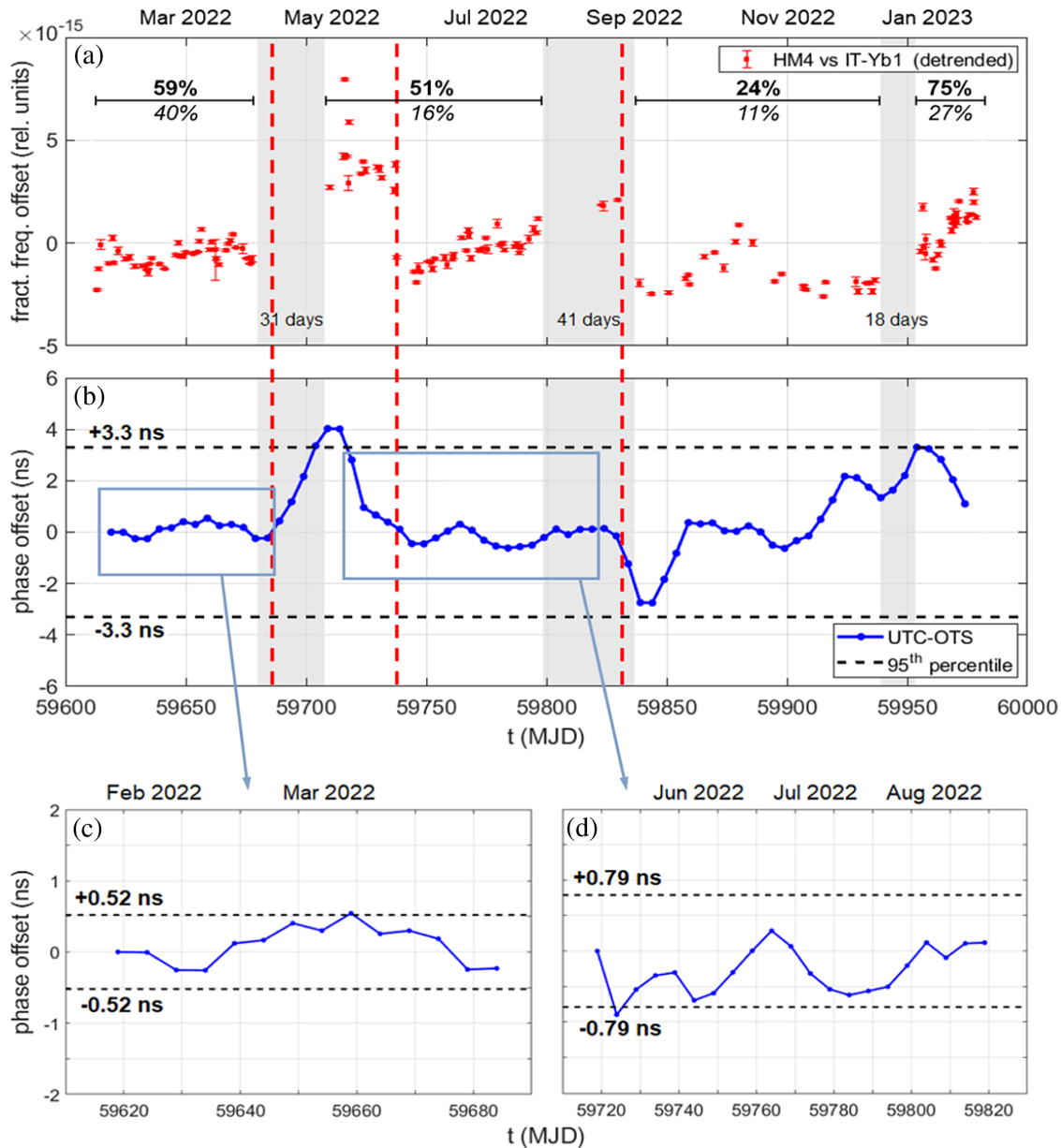


**Fig. 2.** (a) Daily averaged frequency measurements of HM4 versus IT-Yb1 from February 2022 to January 2023. Three major data gaps, with durations of 31, 41, and 18 days, are indicated by the gray-shaded regions. A few measurement data are actually visible within the 41-day gap, but, as these remain isolated from the other more regular measurements, we indicated a unique 41-day gap rather than a gap of 26 days immediately followed by a shorter gap of 8 days. Bold numbers indicate the up-time as percentage of days with at least one measurement whereas italic numbers indicate the up-time according to the classical definition. The three vertical dashed red lines indicate HM4 anomalies. (b) Paper OTS from 9 February 2022 to 30 January 2023, as obtained from the data in panel (a). (c) Zoom-in on the paper OTS within the period highlighted by the first rectangle in panel (b). (d) Paper OTS re-generated in post-processing within the period highlighted by the second rectangle in panel (b).

reported as a bold number. Within the context of our experiment, the above definition of up-time is justified as we update the steering correction only once per day, and we are most interested in the distribution of the daily reporting periods rather than the actual duration of each measurement. However, for the sake of completeness and for an easier comparison with other published results, we also report the up-time as usually defined, i.e., as the percentage of time during which the optical clock is actually taking measurements within the considered period. Within the figure, such a “classical” up-time is reported in italic font. Note that the classical up-time is much lower than the one obtained with our alternative definition, as each daily measurement typically lasts only a small fraction of a day. Over the whole 12-month period, it is about 16%. In addition, note that the IT-Yb1 measurements for this experiment are carried out during working days only; therefore, the maximum expected up-time in a week is approximately 70%.

Figure 2(b) shows the time offset between the paper OTS and UTC, obtained as  $[UTC - UTC(IT)] + [UTC(IT) - OTS]$ . The dashed horizontal lines represent the 95th percentile computed over the whole 1-year period, which is 3.3 ns. This value is strongly influenced by the two peaks occurring around MJD 59,709 and 59,839, which are determined by the simultaneous occurrence of unpredictable anomalies affecting the frequency of HM4 and long-lasting unavailability of IT-Yb1 (31 and 41 days, respectively). In the former case, HM4 changes its frequency slightly after the beginning of the data gap, around the epoch indicated by the first vertical dashed red line, so that the extrapolated steering correction becomes less accurate and the paper OTS soon starts to diverge from UTC, until IT-Yb1 becomes available again. Note that, after the end of the gap, the effect of the  $\Delta f_2$  time accuracy component brings the paper OTS back towards zero. For comparison, also note that around one month after the end of the gap, at the epoch indicated by the second vertical dashed red line, the frequency of HM4 is affected by a jump with amplitude of

some units in  $10^{-15}$  (fractional frequency offset), but in this case the steering correction is properly updated, and the paper OTS remains almost flat around zero offset from UTC, as the frequency change of HM4 occurs during a period with relatively high up-time of the optical clock. Finally, in the case of the 41-day gap, it can be inferred from the few isolated measurements collected within the gap that the frequency of the H maser suffers from another jump at the very end of the gap, around the epoch indicated by the third vertical dashed red line. As a consequence, the accuracy of the extrapolated steering correction remains acceptable for most of the gap duration, and the paper OTS remains almost flat for the major part of the gap, until the HM4 jump causes the OTS to diverge from UTC.

As expected, the paper OTS shows much better performances over the periods with higher up-time of the optical clock. In particular, we focus our attention on the two regions highlighted by the rectangular boxes, characterized by an up-time of 59% and 51%, respectively. A detail of the paper OTS within the first of these regions is shown in Fig. 2(c): the 95th percentile of the time offset, over the whole 2-month period, is as low as 520 ps, which also roughly corresponds to the maximum time offset reached within such a period. The situation is similar for the period considered in panel Fig. 2(d). Here, for a consistent comparison, we re-generated and re-initialized the paper OTS in post-processing, to remove the initial time offset accumulated during the above-described 31-day data gap. Note that the period extends by 20 days into the 41-day gap, during which the steering correction was still good, as can be seen in the second rectangular box of Fig. 2(b). The resulting paper OTS remains well within  $\pm 1$  ns from UTC for the whole 100-day period, with a 95th percentile as low as 790 ps, despite the presence of a frequency jump affecting HM4 around MJD 59740 (second vertical dashed red line), which is properly tracked by the IT-Yb1 measurements and managed by the steering algorithm.

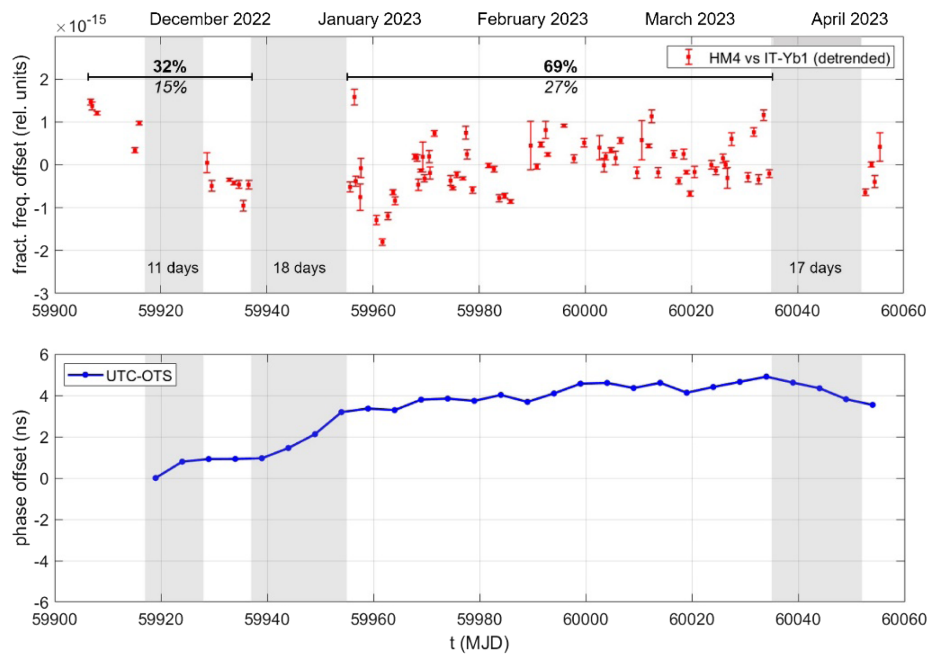


**Fig. 3.** Top: daily averaged frequency measurements of HM4 versus IT-Yb1 from December 2022 to April 2023. Three major data gaps, with durations of 11, 18, and 17 days, are indicated by the gray shaded regions. Bold numbers indicate the up-time as the percentage of days with at least one measurement over the periods indicated by the horizontal bars, whereas italic numbers indicate the up-time according to the classical definition, over the same periods. Bottom: physical OTS from 6 December 2022 to 20 April 2023.

Overall, the paper time scale results demonstrate the possibility to generate a months-long optical time scale with sub-nanosecond accuracy, and the capability to extend such an accuracy to year-long periods, provided that the optical clock up-time is sufficiently high, or the measurements sufficiently regular, to track the occasional non-stationarities of the flywheel's frequency.

## B. Physical Optical Time Scale Results

The physical OTS generation started in December 2022 and ended in the second half of April 2023. During such a period, the physical OTS signal was continuously generated and monitored at the INRiM Time and Frequency laboratory, by using dedicated hardware, as reported in [Supplement 1, Section 1](#).

For this physical OTS realization, we compute  $\Delta f_0$  with  $N_{\text{fit}} = 20$  days. This  $N_{\text{fit}}$  value, smaller than the one of the paper OTS case, guarantees a quicker reaction of the steering algorithm to any possible non-stationarity of the H maser clock frequency, as discussed in [37]. Moreover, as we are primarily interested in assessing the performance of an OTS based on optical clock data only, for this test we set  $\Delta f_2 = 0$ .

Figure 3 shows the results of the physical OTS. The top panel reports the daily-averaged frequency offset data of HM4 versus IT-Yb1 after removing a linear frequency drift of approximately  $5 \times 10^{-16}$ /day over the whole considered period. Data gaps larger than 10 days are indicated by gray-shaded regions. The optical clock up-time is also reported for selected periods, with the same

convention used in Fig. 2, i.e., bold font for the percentage of days with at least one measurement, and italic font for the effective percentage of measuring time. The bottom panel shows the time offset between the physical OTS and UTC. It can be seen that the physical OTS accumulates less than 5 ns with respect to UTC over the whole period and, most importantly, the larger part of the time offset is accumulated during the 18-day data gap, when an unpredictable fluctuation of the frequency of HM4 worsened the accuracy of the extrapolated steering correction. On the contrary, the time offset accumulated in the subsequent 3 months, characterized by a relatively high up-time of IT-Yb1, is less than 2 ns. Note that, in this period, the time accuracy of the physical OTS remains around approximately 4 ns, because the  $\Delta f_2$  component for the time accuracy correction is set to zero. This accumulated time offset demonstrates that relying solely on optical clock data to generate an OTS synchronized to UTC is not sufficient. Therefore, we generate a paper replica of the physical OTS including the time accuracy correction, by computing the  $\Delta f_2$  component from UTCr with  $N_{\text{acc}} = 20$  days, the same value used in the paper OTS discussed in Section 5.A.

As a first step, we validate the procedure for the realization of a paper time scale, by comparing the paper OTS replica, obtained in post-processing with  $\Delta f_2 = 0$ , against the physical OTS, generated in real-time. The successful results of this validation are discussed in [Supplement 1, Section 2](#). Second, we generate the paper OTS replica by including the  $\Delta f_2$  component, based on

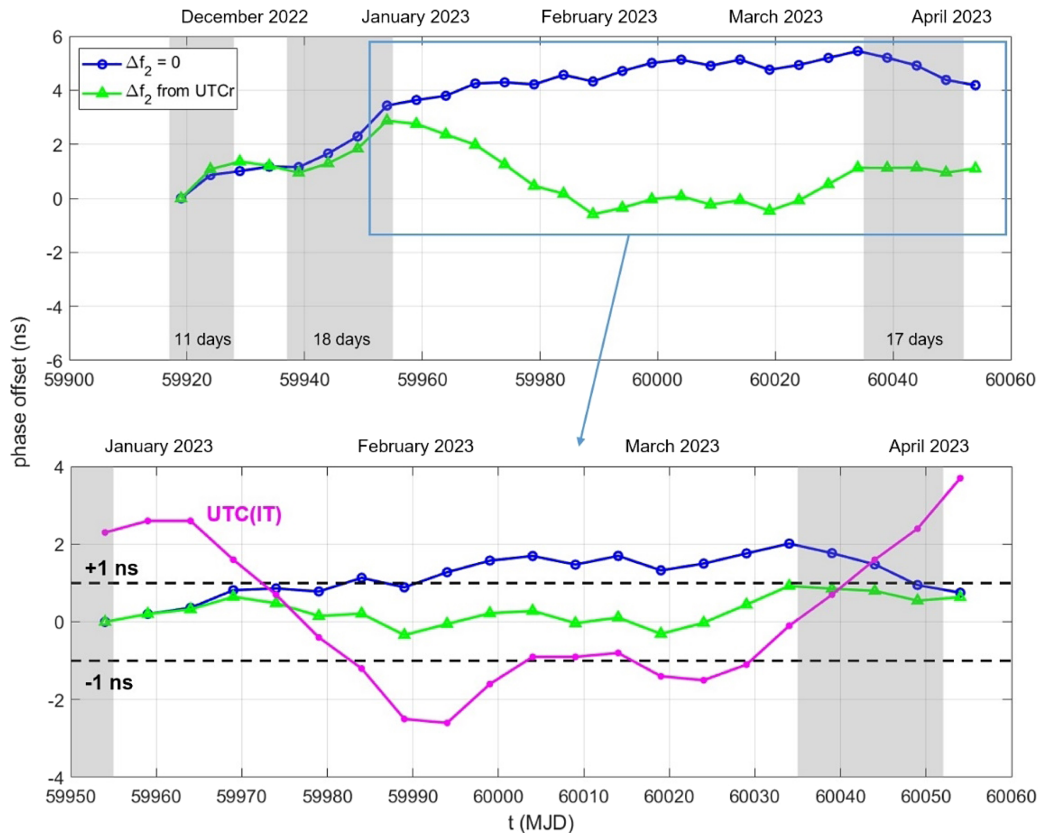


**Fig. 4.** Top: time offset versus UTC of two paper OTS replicas of the physical OTS. The blue line with circles is the paper OTS replica without the  $\Delta f_2$  correction, whereas the green line with triangles is the one with the  $\Delta f_2$  correction based on UTCr, with  $N_{\text{acc}} = 20$  days. Bottom: time offset versus UTC of two paper OTS replicas of the physical OTS, generated for the 3-month period following the 18-day data gap, indicated by the rectangle in the top panel. The color/marker code is the same as for the top panel. The green line with triangles, obtained in this case with  $N_{\text{acc}} = 30$  days, remains well within  $\pm 1$  ns from UTC, as indicated by the horizontal dashed lines. This OTS replica outperforms the Italian time scale UTC(IT) (magenta line with dots). Note that the two time scales are generated by the same master clock (HM4) but with different steering references, i.e., IT-Yb1 for the OTS and UTCr for UTC(IT).

UTCr. The top panel of Fig. 4 shows the obtained paper OTS replicas, namely, the one obtained without the  $\Delta f_2$  correction (blue line with circle markers), and the one with the  $\Delta f_2$  correction (green line with triangle markers). We note that the paper OTS replica with the  $\Delta f_2$  correction properly compensates the time offset accumulated during the 18-day data gap because of the HM4 anomaly. Better performances of the OTS can be obtained in absence of long data gaps and H maser anomalies. As an example, we generate two additional paper OTS replicas, with and without the  $\Delta f_2$  correction, both initialized at the end of the 18-day data gap, that is, after the occurrence of the HM4 non-stationarity. These paper OTS replicas are computed for the period highlighted by the rectangle box in the top panel and are shown in the bottom panel of Fig. 4 (same markers as in the top panel). Since in this period there are no data gaps, for the paper OTS replica with the  $\Delta f_2$  correction we increase the  $N_{\text{acc}}$  parameter to 30 days (instead of 20 days), to further improve its stability. The resulting paper OTS remains well within  $\pm 1$  ns from UTC for the whole 3-month period, demonstrating the potential of a time scale based on an optical clock. This potential is further proved by the comparison against the Italian time scale UTC(IT) (magenta line with dots in the bottom panel), also generated by using HM4 but steered towards UTCr instead of IT-Yb1. As can be seen, the OTS outperforms UTC(IT), which shows much larger fluctuations.

## 6. CONCLUSION

Published research on optical time scales typically reports on experimental time scales with a duration ranging from about 1 to 5 months, during which the optical clock is regularly operated, reaching a sub-nanosecond time accuracy ranging from about 200 to 800 ps [14,15,17,30]. Recently, the performances of a year-long OTS were reported in [19], but in this case, also Cs clocks contribute to the time scale realization, and the overall accuracy is limited to the nanosecond level.

Conversely, the results reported in the present work demonstrate the implementation of a paper and a physical realization of an OTS at INRiM, reaching sub-nanosecond time accuracy over months-long periods and a year-long capability under realistic conditions, including non-stationarities of the flywheel oscillator, weeks-long down-times of the optical clock, and irregularly spaced measurement data.

Moreover, this work paves the way to the systematic inclusion of IT-Yb1 within the ensemble of references routinely used for the robust and automated generation of UTC(IT), along with INRiM cryogenic Cs fountain IT-CsF2, UTC, and UTCr [37]. A promising scenario is the one in which IT-Yb1 and IT-CsF2 data complement themselves by reducing data gaps due to clock down-times. Note that there is still room for improvements from the automation of IT-Yb1 operations, expected to further increase the up-time and reduce the latency with which the measurements are made available to the steering algorithm.

Another interesting result, already obtained in [29] from simulated data and here confirmed by real experimental data, is the importance of performing regular measurements and avoiding large data gaps, which allows the tracking of any possible non-stationarity of the flywheel oscillator and hence reaching sub-nanosecond accuracy even if the total up-time of the optical clock is relatively low.

Finally, we highlight that the experiments discussed in this work demonstrate the possibility to realize robust, stable, and accurate

OTSs, thereby enhancing the realization and dissemination of time scales in line with the future redefinition of the SI second based on an optical transition.

**Funding.** European Metrology Programme for Innovation and Research (EMPIR).

**Acknowledgment.** This work is dedicated to Valerio Formichella, whose expertise, commitment, and passion for research continue to inspire us. This work has been partially carried out within the 18SIB05 ROCIT project, which has received funding from the EMPIR program co-financed by the Participating States and from the European Union's Horizon 2020 research and innovation program.

**Disclosures.** The authors declare no conflicts of interest.

**Data availability.** Data underlying the results presented in this paper are available on Zenodo [39].

**Supplemental document.** See Supplement 1 for supporting content.

## REFERENCES AND NOTES

1. A. D. Ludlow, M. M. Boyd, J. Ye, *et al.*, "Optical atomic clocks," *Rev. Mod. Phys.* **87**, 637–701 (2015).
2. B. J. Bloom, T. L. Nicholson, J. R. Williams, *et al.*, "An optical lattice clock with accuracy and stability at the  $10^{-18}$  level," *Nature* **506**, 71–75 (2014).
3. S. M. Brewer, J.-S. Chen, A. M. Hankin, *et al.*, " $^{27}\text{Al}^+$  quantum-logic clock with a systematic uncertainty below  $10^{-18}$ ," *Phys. Rev. Lett.* **123**, 033201 (2019).
4. J. Grotti, S. Koller, S. Vogt, *et al.*, "Geodesy and metrology with a transportable optical clock," *Nat. Phys.* **14**, 437–441 (2018).
5. M. Takamoto, I. Ushijima, N. Ohmae, *et al.*, "Test of general relativity by a pair of transportable optical lattice clocks," *Nat. Photonics* **14**, 411–415 (2020).
6. R. Lange, N. Huntemann, J. M. Rahm, *et al.*, "Improved limits for violations of local position invariance from atomic clock comparisons," *Phys. Rev. Lett.* **126**, 011102 (2021).
7. N. Dimarcq, M. Gertsolf, G. Mileti, *et al.*, "Roadmap towards the redefinition of the second," *Metrologia* **61**, 012001 (2024).
8. J. Lodewyck, "On a definition of the SI second with a set of optical clock transitions," *Metrologia* **56**, 055009 (2019).
9. Resolutions of the General Conference on Weights and Measures (27th meeting), 15–18 November 2022, published by the BIPM, <https://www.bipm.org/en/cgpm-2022> (URL consulted on February 2024).
10. G. Panfilo and F. Arias, "The coordinated universal time (UTC)," *Metrologia* **56**, 042001 (2019).
11. BIPM webpage for time metrology, <https://www.bipm.org/en/time-metrology> (URL consulted February 2024).
12. F. Riehle, F. Arias, and L. Robertsson, "The CIPM list of recommended frequency standard values: guidelines and procedures," *Metrologia* **55**, 188–200 (2018).
13. H. S. Margolis, G. Panfilo, G. Petit, *et al.*, "The CIPM list 'Recommended values of standard frequencies': 2021 update," *arXiv*, arXiv:2401.14537 (2024).
14. H. Hachisu, F. Nakagawa, Y. Hanado, *et al.*, "Months-long real-time generation of a time scale based on an optical clock," *Sci. Rep.* **8**, 4243 (2018).
15. C. Grebing, A. Al-Masoudi, S. Dörscher, *et al.*, "Realization of a timescale with an accurate optical lattice clock," *Optica* **3**, 563–569 (2016).
16. J. Yao, T. E. Parker, N. Ashby, *et al.*, "Incorporating an optical clock into a time scale," *IEEE Trans. Ultrason. Ferroelectr. Freq. Control* **65**, 127–134 (2018).
17. J. Yao, J. A. Sherman, T. Fortier, *et al.*, "Optical-clock-based time scale," *Phys. Rev. Appl.* **12**, 044069 (2019).
18. M. Abgrall, B. Chupin, U. L. Lorini, *et al.*, "Optically steered time scale generation at OP and NPL and remote comparisons," in *The 9th Symposium on Frequency Standards and Metrology* (2023).
19. H. Hachisu, H. Ito, N. Nemitz, *et al.*, "UTC(NICT) referenced to a timescale based on the optical clock NICT-Sr1," in *Proceedings Joint Conference of the European Frequency and Time Forum and IEEE International Frequency Control Symposium* (2023).

20. W. R. Milner, J. M. Robinson, C. J. Kennedy, *et al.*, "Demonstration of a timescale based on a stable optical carrier," *Phys. Rev. Lett.* **123**, 173201 (2019).
21. J. Lodewyck, S. Bilicki, E. Bookjans, *et al.*, "Optical to microwave clock frequency ratios with a nearly continuous strontium optical lattice clock," *Metrologia* **53**, 1123 (2016).
22. T. Kobayashi, D. Akamatsu, K. Hosaka, *et al.*, "Demonstration of the nearly continuous operation of an  $^{171}\text{Yb}$  optical lattice clock for half a year," *Metrologia* **57**, 065021 (2020).
23. C. F. A. Baynham, R. M. Godun, J. M. Jones, *et al.*, "Absolute frequency measurement of the optical clock transition in with an uncertainty of using a frequency link to international atomic time," *J. Mod. Opt.* **65**, 585–591 (2017).
24. R. Hobson, W. Bowden, A. Vianello, *et al.*, "A strontium optical lattice clock with  $1 \times 10^{-17}$  uncertainty and measurement of its absolute frequency," *Metrologia* **57**, 065026 (2020).
25. H. Kim, M.-S. Heo, C. Y. Park, *et al.*, "Absolute frequency measurement of the  $^{171}\text{Yb}$  optical lattice clock at KRISS using TAI for over a year," *Metrologia* **58**, 055007 (2021).
26. W. F. McGrew, X. Zhang, H. Leopardi, *et al.*, "Towards the optical second: verifying optical clocks at the SI limit," *Optica* **6**, 448–454 (2019).
27. N. Nemitz, T. Gotoh, F. Nakagawa, *et al.*, "Absolute frequency of  $^{87}\text{Sr}$  at  $1.8 \times 10^{-16}$  uncertainty by reference to remote primary frequency standards," *Metrologia* **58**, 025006 (2021).
28. D. Herman, S. Droste, E. Baumann, *et al.*, "Femtosecond timekeeping: slip-free clockwork for optical timescales," *Phys. Rev. Appl.* **9**, 044002 (2018).
29. V. Formichella, L. Galleani, G. Signorile, *et al.*, "Robustness tests for an optical time scale," *Metrologia* **59**, 015002 (2022).
30. L. Zhu, Y. Lin, Y. Wang, *et al.*, "Preliminary study of generating a local time scale with NIM  $^{87}\text{Sr}$  optical lattice clock," *Metrologia* **59**, 055007 (2022).
31. I. Goti, S. Condio, C. Clivati, *et al.*, "Absolute frequency measurement of a Yb optical clock at the limit of the Cs fountain," *Metrologia* **60**, 035002 (2023).
32. V. Formichella, G. Signorile, T. T. Thai, *et al.*, "Reliable and robust real-time time scale generation: developments and experimental results at INRiM," in *Proceedings 2020 Precise Time and Time Interval System and Applications Meeting* (2020).
33. A. Perucca, T. T. Thai, F. Fiasca, *et al.*, "Network and software architecture improvements for a highly automated, robust and efficient realization of the Italian national time scale," in *Proceedings 2021 Joint Conference of the European Frequency and Time Forum and IEEE International Frequency Control Symposium* (2021).
34. "iMaser 3000 specifications," <https://www.t4science.ch/products/imaser3000> (URL consulted on February 2024).
35. M. Pizzocaro, F. Bregolin, B. Rauf, *et al.*, "Absolute frequency measurement of the  $^1\text{S}_0\text{-}^3\text{P}_0$  transition of  $^{171}\text{Yb}$  with a link to international atomic time," *Metrologia* **57**, 035007 (2020).
36. M. Pizzocaro, B. Rauf, F. Bregolin, *et al.*, "Absolute frequency measurement of the  $^1\text{S}_0\text{-}^3\text{P}_0$  transition of  $^{171}\text{Yb}$ ," *Metrologia* **54**, 102–112 (2017).
37. L. Galleani, G. Signorile, V. Formichella, *et al.*, "Generating a real-time time scale making full use of the available frequency standards," *Metrologia* **57**, 065015 (2020).
38. G. Petit, F. Arias, A. Harmegnies, *et al.*, "UTCr: a rapid realization of UTC," *Metrologia* **51**, 33 (2013).
39. V. Formichella, G. Signorile, T. T. Thai, *et al.*, "Year-long optical time scale with sub-nanosecond capabilities," Zenodo, 2024, <https://zenodo.org/doi/10.5281/zenodo.10880674>.